Q-switched thulium-doped fibre laser operating at 1900 nm using multi-walled carbon nanotubes saturable absorber

Norazlina Saidin[1,2,3], Dess I.M. Zen[1,4], Fauzan Ahmad[1,2], Hazlihan Haris[1], Muhammad T. Ahmad[1,5], Anas A. Latiff[5], Harith Ahmad[1], Kaharudin Dimyati[4], Sulaiman W. Harun[1,2]

[1]*Photonics Research Centre, University of Malaya, 50603 Kuala Lumpur, Malaysia*
[2]*Department of Electrical Engineering, Faculty of Engineering, University of Malaya, 50603 Kuala Lumpur, Malaysia*
[3]*Department of Electrical and Computer Engineering, International Islamic University Malaysia, Jalan Gombak, 53100 Kuala Lumpur, Malaysia*
[4]*Department of Electrical and Electronic Engineering, National Defense University of Malaysia, Kem Sungai Besi, 57000 Kuala Lumpur, Malaysia*
[5]*Faculty of Electronic and Computer Engineering, Universiti Teknikal Malaysia Melaka, 76100 Durian Tunggal, Melaka, Malaysia*
E-mail: swharun@um.edu.my

Published in *The Journal of Engineering*; Received on 3rd February 2014; Accepted on 19th May 2014

Abstract: Simple, low-cost and stable passive Q-switched thulium-doped fibre lasers (TDFLs) operating at 1892.4 and 1910.8 nm are demonstrated using 802 and 1552 nm pumping schemes, respectively, in conjunction with a multi-walled carbon nanotubes (MWCNTs) saturable absorber (SA). The MWCNTs composite is prepared by mixing the MWCNTs homogeneous solution into a dilute polyvinyl alcohol (PVA) polymer solution before it is left to dry at room temperature to produce thin film. Then the film is sandwiched between two FC/PC fibre connectors and integrated into the laser cavity for Q-switching pulse generation. The pulse repetition rate of the TDFL configured with 802 nm pump can be tuned from 3.8 to 4.6 kHz, whereas the corresponding pulse width reduces from 22.1 to 18.3 μs as the pump power is increased from 187.3 to 194.2 mW. On the other hand, with 1552 nm pumping, the TDFL generates optical pulse train with a repetition rate ranging from 13.1 to 21.7 kHz with a pulse width of 11.5–7.9 μs when the pump power is tuned from 302.2 to 382.1 mW. A higher performance Q-switched TDFL is expected to be achieved with the optimisation of the MWCNT-SA saturable absorber and laser cavity.

1 Introduction

Q-switched fibre-based laser systems operating in the 'eye-safe' wavelength of 1900 nm region are promising for applications such as light detection and ranging (lidar), differential absorption lidar and as pumps for mid-IR generation. They can be realised using thulium-doped or holmium-doped fibre lasers based on either active or passive methods [1–3]. Compared with the active ones, passively Q-switched fibre lasers feature flexibility of configuration and do not require additional switching electronics. These lasers have been successfully demonstrated using different kinds of saturable absorbers (SAs), such as semiconductor SA mirrors (SESAMs) [3, 4] and single-wall carbon nanotubes (SWCNTs) [5, 6]. However, SESAMs are still expensive and complex to be fabricated. Therefore, more focus has been given on the utilisation of SWCNTs as an SA in recent years especially for all-fibre Q-switched and mode-locked fiber lasers [7–9]. This is because of their inherent advantages, including good compatibility with optical fibers, low saturation intensity, fast recovery time and wide operating bandwidth.

Recently, a new member of carbon nanotubes family, multi-walled carbon nanotubes (MWCNTs) [10, 11] have also attracted many attentions for non-linear optics applications because of their production cost, which is about 50–20% of that of SWCNT material [12]. The growth of the MWCNT material does not need complicated techniques or special growing conditions so that its production yield is high for each growth. Compared with SWCNTs, the MWCNTs have higher mechanical strength, better thermal stability as well as can absorb more photons per nanotube because of its higher mass density of the multi-walls. These favourable features are because of the structure of MWCNTs which take the form of a stack of concentrically rolled graphene sheets. The outer walls can protect the inner walls from damage or oxidation so that the thermal or laser damage threshold of MWCNT is higher than that of the SWCNTs [13, 14]. To date, there are only a few reported works on application of MWCNTs material as an SA. For instance, Zhang *et al.* [12] employs multi-walled MWCNTs based SA for mode locking of an Nd:YVO_4 laser. In another work, Q-switched Nd-YAG laser is demonstrated using the MWCNTs based SA as a Q-switcher.

In this paper, an all-fibre Q-switched thulium-doped fibre laser (TDFL) is demonstrated using a simple and low-cost newly developed MWCNTs based SA as the Q-switcher. The SA employs MWCNTs-polyvinyl alcohol (PVA) film, which is fabricated by mixing a dispersed MWCNTs suspension into a PVA solution. The SA is integrated in the TDFL by sandwiching the film between two fibre connectors that results in a stable pulse train with 4.6 kHz repetition rate, 18.3 μs pulse width and 126.1 nJ pulse energy at 194.2 mW 802 nm pump power. The performance of the TDFL is also investigated with 1552 nm pumping, whereby a stable pulse train with 21.7 kHz repetition rate, 7.9 μs pulse width and 103.4 nJ pulse energy at 382.1 mW pump power.

2 Fabrication and Raman characterisation of MWCNT-PVA film

The MWCNTs material used for the fabrication of the absorber in this experiment is functionalised so that it can be dissolved in water. The diameter of the MWCNTs used is about 10–20 nm and the length distribution is from 1 to 2 μm. The functionaliser solution was prepared by dissolving 4 g of sodium dodecyl sulphate in 400 ml deionised water. About 250 mg MWCNT was added to the solution and the homogenous dispersion of MWCNTs was achieved after the mixed solution was sonicated for 60 min at 50 W. The solution was then centrifuged at 1000 rpm to remove large particles of undispersed MWCNTs to obtain dispersed suspension that is stable

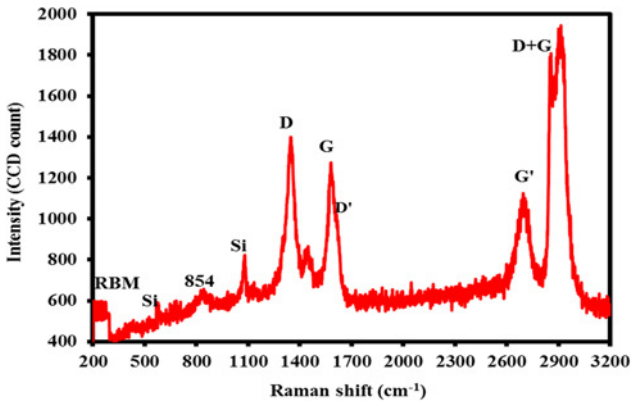

Fig. 1 *Raman spectrum obtained from the MWCNTs-PVA film*

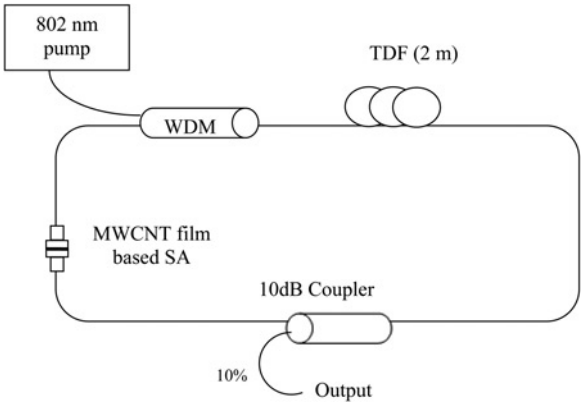

Fig. 3 *Schematic configuration of the Q-switched TDFL with 802 nm pumping*

for weeks. MWCNTs-PVA composite was prepared by adding the dispersed MWCNTs suspension into a PVA solution by a three to two ratio. Solution was prepared by dissolving 1 g of PVA (M_w = 89×10^3 g/mol) in 120 ml of deionised water. The homogeneous MWCNTs-PVA composite was obtained by a sonification process for more than one hour. The composite was casted onto a glass petri dish and left to dry at room temperature for about one week to produce thin film with a thickness of around 50 µm.

Raman spectroscopy was performed on the prepared MWCNT-PVA film using laser excitation at 532 nm to confirm the presence of the carbon nanotubes. Fig. 1 shows the Raman spectrum, obviously indicating the distinct feature of the MWCNT. It is shown that the Raman spectrum bears a lot of similarity to graphene, which is not too surprising as it is simply a rolled up sheet of graphene. MWCNT has many layers of graphene wrapped around the core tube. We can see well defined G (1580 cm^{-1}) and G' (2705 cm^{-1}) bands in Fig. 1 as there were in graphene and graphite. The G-band originates from in-plane tangential stretching of the carbon–carbon bonds in graphene sheet. We also see a prominent band around 1350 cm^{-1}, which is known as the D-band. The D-band originates from a hybridised vibrational mode associated with graphene edges and it indicates the presence of some disorder to the graphene structure. This band is often referred to as the disorder band or the defect band and its intensity relative to that of the G-band is often used as a measure of the quality with nanotubes. There is another series of bands appearing at the low-frequency end of the spectrum known as radial breathing mode bands. These bands correspond to the expansion and contraction of the tubes and are not clearly present in the MWCNT because of the outer tubes, which restrict the breathing mode. As expected, the prominent D-band is observed in Fig. 1, indicating the nanotubes as a multi-walled type, which has multi-layer configuration and disorder structure. The D'-band which is a weak shoulder of the G-band is also observed at 1613 cm^{-1} because of double resonance feature induced by disorder and defect. In addition, other distinguishable features like D + G band (2920 cm^{-1}), a small peak at 854 cm^{-1} and Si were also observed as depicted in Fig. 1. Fig. 2 shows the transmission spectrum of the fabricated MWCNTs-PVA film. As shown in the figure, the transmission is featureless in the near infra-red region, showing the broadband property of our SA. The transmittance is observed to be about 50.8% at 1900 nm region.

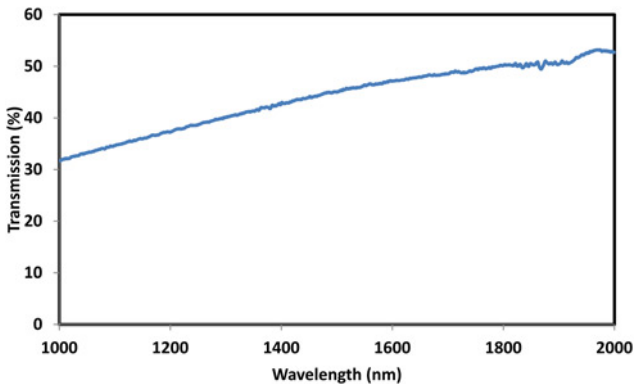

Fig. 2 *Transmission spectrum of the MWCNTs-PVA film*

3 Configuration of the laser

The schematic of the proposed Q-switched TDFL is shown in Fig. 3. It was constructed using a simple ring cavity, in which a 2 m long TDF with absorption of 27 dB/m at 785 nm was used for the active medium and the fabricated MWCNT-based SA was used as a Q-switcher. The SA is fabricated by cutting a small part of the prepared MWCNTs-PVA film and sandwiching it between two ferrule connector/physical contact (FC/PC) fibre connectors, after depositing an index-matching gel onto the fibre ends. Figs. 4*a* and *b* show the image of the film attached onto a fibre ferule and the constructed SA, respectively. The insertion loss of the SA is measured to be around 3.3 dB at 1900 nm. The thalium-doped fibre (TDF) was pumped by an 802 nm laser diode via an 800/2000 nm wavelength division multiplexer (WDM). The temporal characteristics of the laser output were monitored using a combination of a photo-detector and a real-time oscilloscope. The optical spectrum was measured using an optical spectrum analyser. The cavity length is measured to be ~7.6 m. The performance of the Q-switched TDFL is also investigated for 1552 nm pumping. In the experiment, 802 nm laser diode and 800/2000 nm WDM are replaced with 1552 nm pump and 1550/1900 nm WDM, whereas the TDF length is increased to 5 m for optimum laser performance.

4 Q-switching performance with 802 nm pumping

Fig. 5 shows the output power of both Q-switched and continuous wave (CW) lasers against the input pump power, which are obtained with and without the SA, respectively. Without the SA, a CW laser operates with an efficiency of 3.77% and threshold pump power of 133.1 mW. The efficiency is relatively low since the components used have a considerably high insertion loss at 1900 nm region. As the SA is inserted into the ring cavity, a stable and self-starting Q-switching operation is obtained just by adjusting the pump power over a threshold of 187.3 mW. However, the efficiency of the laser is slightly reduced to 2.68% because of the increased cavity loss. Fig. 6 shows the output spectrum of the TDFL with and without SA at the pump power

doi: 10.1049/joe.2014.0038

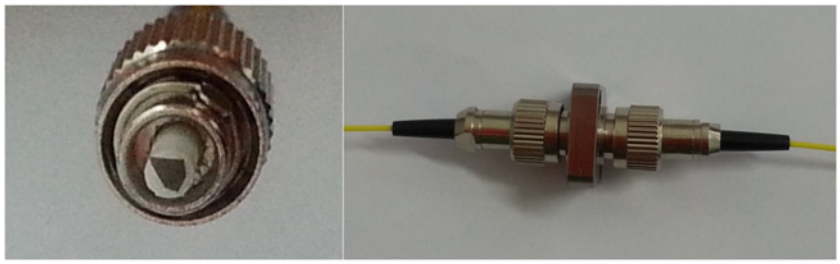

Fig. 4 *MWCNTs-PVA film-based SA*
a Attachment of the film on the fibre ferrule
b Integration of MWCNT composite film in laser cavity

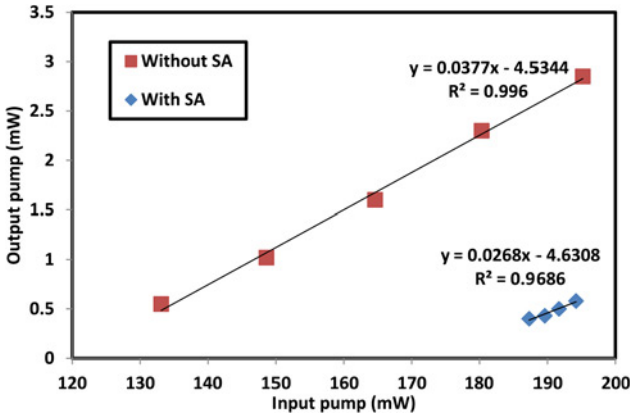

Fig. 5 *Output power characteristic against the pump power with and without the SA*

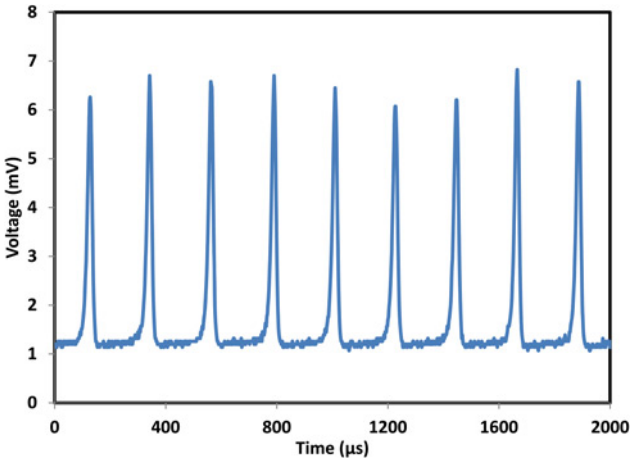

Fig. 7 *Q-switching pulse train at the pump power of 191.7 mW*

threshold of 187.3 mW. As can be seen from the figure, the Q-switched laser operates at a wavelength of 1892.4 nm with an optical signal-to-noise ratio (SNR) of more than 30 dB. Compared with the CW laser (without SA), the operating wavelength of the Q-switched laser has shifted to a shorter wavelength. This is attributed to the cavity loss which increases with the incorporation of SA. Thus, the oscillating light in the cavity shifts to a shorter wavelength, which is closer to the peak absorption of the TDF at around 1800 nm to compensate for the loss. The spectrum bandwidth is also broadened in the Q-switched laser because of the self-phase modulation effect in the ring cavity.

Fig. 7 shows the oscilloscope trace of the Q-switched pulse train at the pump power of 191.7 mW. As shown in the figure, there is no distinct amplitude modulation in each Q-switched envelope spectrum, which means that the self-mode locking effect on the Q-switching is weak. At this pump power, the proposed TDFL generates a stable Q-switching pulse with an average output power of 0.5 mW and repetition rate of 4.5 kHz. The pulse energy is calculated to be around 111.1 nJ at this pump power. The pulse energy

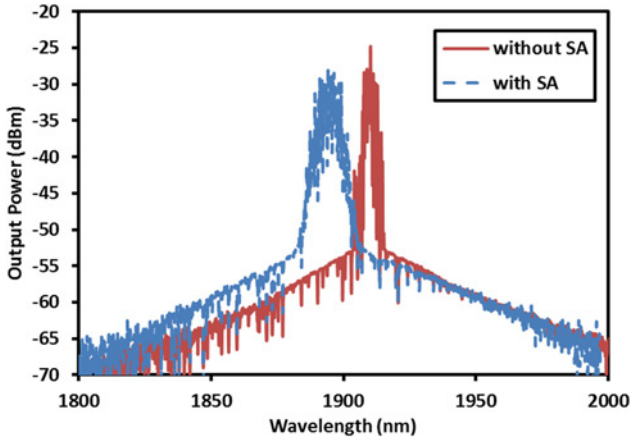

Fig. 6 *Output spectrum of the ring TDFL with and without the SA*

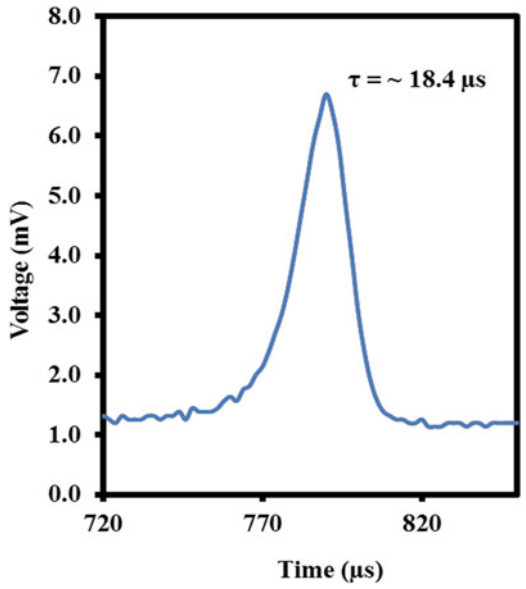

Fig. 8 *Pulse envelope of the Q-switched laser at the pump power of 191.7 mW*

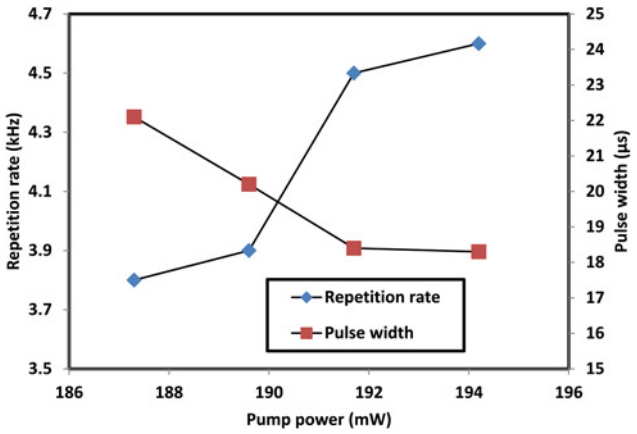

Fig. 9 *Repetition rate and pulse width as a function of pump power*

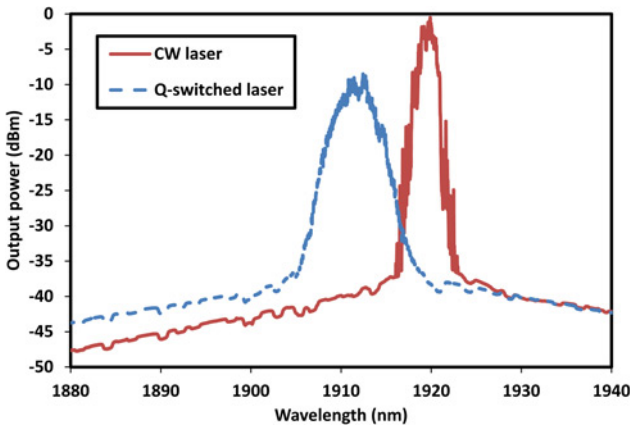

Fig. 11 *Optical spectra of the TDFL with CW and Q-switching modes of operation*

could be improved by reducing the insertion loss of the SA and optimising the laser cavity. Fig. 8 shows the typical oscilloscope trace of the pulse envelop at the pump power of 191.7 mW. As seen in the figure, the full-width at half-maximum (FWHM) or pulse width was obtained at 18.4 μs.

Fig. 9 shows the repetition rate and the pulse width of the proposed Q-switched TDFL against the pump power. The repetition rate has a monotonically increasing, near-linear relationship with the pump power level, which is consistent with other reported results of the SWCNT-based fibre lasers [8]. When the pump power is tuned from 187.3 to 194.2 mW, the pulse train repetition rate varies from 3.8 to 4.6 kHz. On the other hand, the pulse width is inversely proportional to the pump power, where the pulse duration becomes shorter as the pump power increases. The shortest pulse width of 18.3 μs is achieved at the maximum pump power of 194.2 mW. The pulse width is expected to decrease further if the pump power can be augmented beyond 194.2 mW as long as it is still kept below the damage threshold of the MWCNT-PVA-based SA. Shortening the total cavity length of the fibre laser is another alternative to obtain a shorter pulse. Fig. 10 shows the output power and pulse energy as functions of pump power. It is found that both output pump power and pulse energy increase with the pump power. At the maximum pump power of 194.2 mW, the average pump power and pulse energy of the Q-switched laser are obtained at 0.58 mW and 126.1 nJ.

5 Q-switching performance with 1552 nm pumping

Aside from 802 nm pumping, the TDFL can also be pumped by 1552 nm light to create a population inversion between $^3F_4$ and $^3H_6$ energy levels and generates laser at 1900 nm region. Here, the performance of the Q-switched TDFL is investigated using a 1552 nm pump as the pump source based on the similar setup of Fig. 3. The total cavity length is measured to be around 11.6 m because of the increment of both TDF and WDM fibre lengths. Without the SA in the cavity, the TDFL starts to operate in CW mode at threshold pump power of 256 mW. As the SA is incorporated into the cavity, a stable self-started Q-switching pulse train is obtained at the slightly higher pump power of 302.2 nm than the CW operation. Fig. 11 compares the optical spectrum of the Q-switched TDFL with the CW one, which was obtained by removing the SA. Both lasers operate at a longer wavelength compared with the previous TDFL configured with 802 nm pumping because of the longer TDF length used. The longer TDF provides a higher population inversion and thus shifts the operating wavelength to a longer wavelength region. The Q-switched TDFL operates at wavelength of 1910.8 nm, which is slightly shorter than the CW laser owing to the insertion loss in the SA. It has a broad FWHM of 3.0 nm because of the self-phase modulation (SPM) effect in the ring cavity and SNR of ~30 dB.

Fig. 12 shows the oscilloscope trace of the typical Q-switched pulse train at 1552 nm pump power of 382.1 mW. It is observed that the Q-switching operation is stable for the TDFL where neither amplitude variation nor timing jitter was notable in the pulse train. The spacing between two pulses in Fig. 12 is measured to be around 46.0 μs, which can be translated to repetition rate of 21.7 kHz. At this pump power, the pulse width and average pump power were measured to be 7.9 μs and 2.2 mW, respectively, and thus the pulse energy is calculated to be 103.4 nJ. Fig. 13 shows how repetition rate and pulse width are related to the pump power

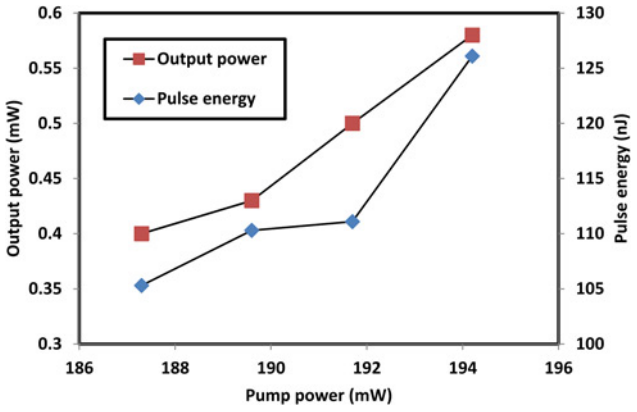

Fig. 10 *Average output power and pulse energy as a function of pump power*

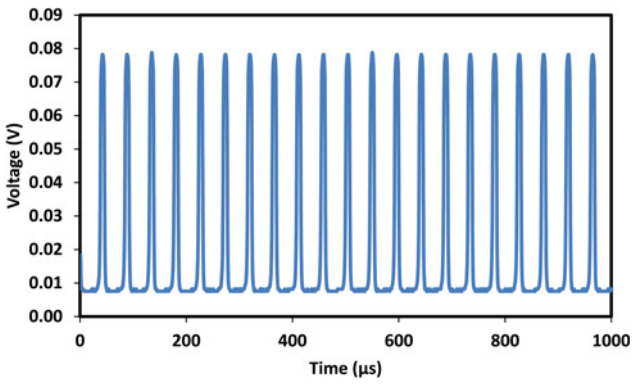

Fig. 12 *Typical pulse train for the proposed TDFL at 1552 nm pump power of 382.1 mW*

doi: 10.1049/joe.2014.0038

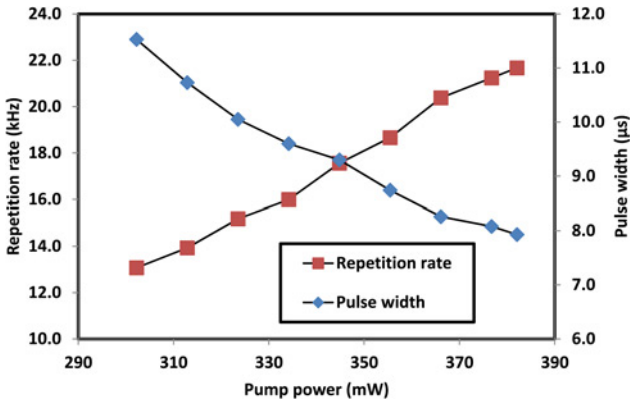

Fig. 13 *Repetition rate and pulse width as a function of 1552 nm pump power*

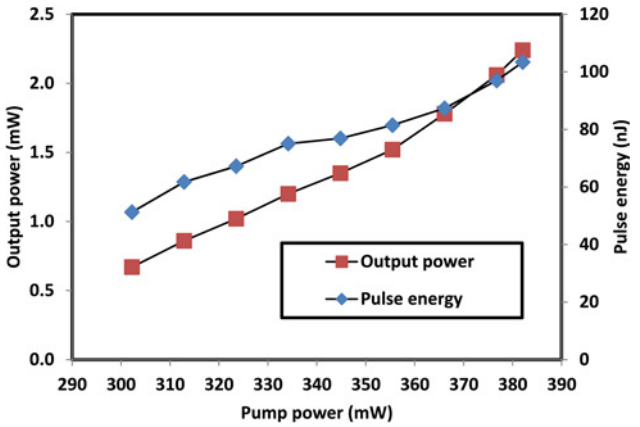

Fig. 14 *Average output power and pulse energy as a function of 1552 nm pump power*

for the TDFL. In the laser, the dependence of the pulse repetition rate can be seen to increase almost linearly with the pump power, whereas the pulse width decreases also almost linearly with the pump power. This agrees well with the previous result on 802 nm pumping. By varying the pump power from 302.2 to 382.1 mW, the pulse repetition rate of the Q-switched TDFL configured with 1552 nm pumping can be widely tuned from 13.1 to 21.7 kHz, whereas the corresponding pulse width reduces from 11.5 to 7.9 μs. The Q-switching pulse becomes unstable and disappeared as the pump power increases above 382.1 mW.

Fig. 14 shows the average output power and pulse energy of the proposed Q-switched TDFL as a function of 1552 nm pump power. It is observed that both output power and pulse energy increase with the increment of the pump power from 302.2 to 382.1 mW. Further increasing the pump power leads to randomising the pulses and the pulse train of the passively Q-switched laser became unstable and strong amplitude variation appeared. It is predicted that the fluctuation is caused by the lower damage threshold of the MWCNT under higher pump power, considering the fact that the laser will completely stop lasing if the pump power is further increased. It is also observed that the Q-switching operation of the laser can be resumed back as the pump power is reduced within 302.2–382.1 mW. At the maximum pump power of 382.1 mW, the TDFL produces the highest average output power and pulse energy of 2.2 mW and 103.4 nJ, respectively. These results indicate that both 802 and 1552 nm pumping schemes can be used for generating Q-switching pulse train in the TDFL. It is also shown that the MWCNTs-PVA SA has a big potential for superior Q-switching and saturable absorption compared with conventional light absorbing components when carefully employed in an appropriate laser system. The fabrication of the SA is also simple and thus the cost of the laser should be low. The simple and low cost laser is suitable for applications in metrology, environmental sensing and biomedical diagnostics.

6 Conclusion

A stable passive Q-switched TDFL operating at 1900 nm region is successfully demonstrated using 802 and 1552 nm pumping schemes, in conjunction with MWCNTs-SA. The SA employs MWCNT film, which is fabricated by mixing the MWCNTs homogeneous solution into a PVA polymer solution. With 1552 nm pumping, the average output power, repetition rate and pulse width are obtained at 2.2 mW, 21.7 kHz and 7.9 μs, respectively, when the pump power is fixed at 382.1 mW. As compared with the 802 nm pumping, these performances are better, which can be accounted from the higher pump power applied to the TDF. The Q-switched TDFL configured by 802 nm pump gives the pulse width, repetition rate and output power of 18.3 μs, 4.6 kHz and 0.58 mW, respectively, when the pump power is 194.2 mW. The highest pulse energy of 126.1 nJ is also obtained at this pump power.

7 Acknowledgment

This work is financially supported by Ministry of Education and University of Malaya under various grant schemes (Grant Numbers: PG139-2012B, ER012-2012A, RP008D-13AET and RP008C-13AET).

8 References

[1] El-Sherif A.F., King T.A.: 'High-energy, high-brightness Q-switched Tm^{3+}-doped fiber laser using an electro-optic modulator', *Opt. Commun.*, 2003, **218**, (4–6), pp. 337–344
[2] Jiang M., Ma H.F., Ren Z.Y., *ET AL.*: 'A graphene Q-switched nanosecond Tm-doped fiber laser at 2 μm', *Laser Phys. Lett.*, 2013, **10**, (5), p. 055103
[3] Wang Q., Geng J., Jiang Z., Luo T., Jiang S.: 'Mode-locked Tm–Ho-codoped fiber laser at 2.06 μm', *IEEE Photonics Technol. Lett.*, 2011, **23**, pp. 682–684
[4] Kivistö S., Koskinen R., Paajaste J., Jackson S.D., Guina M., Okhotnikov O.G.: 'Passively Q-switched Tm3 +, Ho3 +-doped silica fiber laser using a highly nonlinear saturable absorber and dynamic gain pulse compression', *Opt. Express*, 2008, **16**, (26), p. 22058
[5] Solodyankin M.A., Obraztsova E.D., Lobach A.S., *ET AL.*: 'Mode-locked 1.93 μm thulium fiber laser with a carbon nanotube absorber', *Opt. Lett.*, 2008, **33**, (12), pp. 1336–1338
[6] Kieu K., Wise F.: 'Soliton thulium-doped fiber laser with carbon nanotube saturable absorber', *IEEE Photonics Technol. Lett.*, 2009, **21**, (3), pp. 128–130
[7] Hasan T., Sun Z., Wang F., *ET AL.*: 'Nanotube–polymer composites for ultrafast photonics', *Adv. Mater.*, 2009, **21**, (38-39), pp. 3874–3899
[8] Ahmad F., Harun S., Nor R., Zulkepely N., Ahmad H., Shum P.: 'A passively mode-locked erbium-doped fiber laser based on a single-wall carbon nanotube polymer', *Chin. Phys. Lett.*, 2013, **30**, (5), p. 054210
[9] Harun S.W., Saidin N., Zen D.I.M., *ET AL.*: 'Self-starting harmonic mode-locked thulium-doped fiber laser with carbon nanotubes saturable absorber', *Chin. Phys. Lett.*, 2013, **30**, (9), p. 094204, doi: i10.1088/0256–307x/30/9/094204
[10] Costa S., Borowiak-Palen E., Kruszynska M., Bachmatiuk A., Kalenczuk R.: 'Characterization of carbon nanotubes by Raman spectroscopy', *Mater. Sci. Poland*, 2008, **26**, (2), pp. 433–441
[11] Dresselhaus M.S., Dresselhaus G., Saito R., Jorio A.: 'Raman spectroscopy of carbon nanotubes', *Phys. Rep.*, 2005, **409**, (2), pp. 47–99
[12] Zhang L., Wang Y.G., Yu H.J., *ET AL.*: 'Passive mode-locked Nd: YVO4 laser using a multi-walled carbon nanotube saturable absorber', *Laser Phys.*, 2011, **21**, pp. 1382–1386
[13] Ramadurai K., Cromer C.L., Lewis L.A., *ET AL.*: 'High-performance carbon nanotube coatings for high-power laser radiometry', *J. Appl. Phys.*, 2008, **103**, p. 013103
[14] Banhart F.: 'Irradiation effects in carbon nanostructures', *Rep. Prog. Phys.*, 1999, **62**, p. 1181